

Influence of Internal Couplings in Gaussian and Diagrammatic Approximations for Langevin Dynamics

Report for "Research Methods for Theoretical Modelling of Non Equilibrium Systems" course

Sirio Belga Fedeli^a

^aMSc in Non Equilibrium, CANES program, King's College London, London, United Kingdom
sirio.belga.fedeli@kcl.ac.uk

Abstract

The aim of this work is to test the accuracy of the Gaussian approximation and of the diagrammatic expansion for a multidimensional Langevin equation. A particular emphasis is devoted to the structure of the coupling terms in the dynamics of the model. Numerical solutions provide a qualitative benchmark of investigation and demonstrate that the performances of the methods are extremely affected by the choice of the onset parameters. In particular, as the analysis of the errors for the means and the autocorrelations underline, the symmetry of the interaction matrix and the size of the system are found to play a fundamental role and identify preferential setups.

Keywords: Langevin Dynamics, Gaussian Approximation, Diagrammatic Expansion

1. Introduction

Several systems in nature are dominated by collective behaviour of single entities. Although the latter interact with each other according to simple rules, the macroscopic system exhibits complex patterns and robust schemes. These phenomena can be modelled as a system of stochastic differential equations (SDEs) affected by external and internal sources of noise [1]. Randomness affects the stability and leads the system towards selected configurations, eventually showing phase transitions. Neural networks are example of these non-equilibrium systems since synapses, which connect neurons, exhibit high level of stochasticity and heterogenous firing patterns [2]. The emergence of patterns has relevant implications in ecological systems and their asymptotic stability. Although with some differences, networks of interaction can also be found in social systems [3]. The paper is organised as follows: section 2 provides a brief overview of the mathematical framework, sections 3-4-5 review the methods adopted with particular emphasis on the derivation of the Gaussian and diagrammatic approximations. Section 6, which is the main part of this work, contains a qualitative comparison on the accuracy of the methods for the means and autocorrelations. Lastly contents in section 7 summarise the results achieved and outline further possible investigations.

2. Dynamical Modelling

The state of a system, consisting of N elements, can be identified by the vector $\mathbf{x} = (x_1, x_2, \dots, x_N) \in \mathbb{R}^N$ where each entry x_i represents the state of the element i . Therefore the time evolution of \mathbf{x} can be described by a system of coupled ordinary SDEs of the form:

$$\partial_t x_i = -x_i + \sum_{j \neq i} J_{ij} g(x_j) + \xi_i \quad (1)$$

For any $i = 1, \dots, N$. The structure of the network is encoded within the interaction matrix J_{ij} whose entries are correlated Gaussian variables with zero mean, $\langle J_{ij}^2 \rangle = J^2/N$ while $J_{ii} = 0$. In addition it is assumed for all $i = 1, \dots, N$ that $\langle J_{ij} J_{ji} \rangle = \eta J^2/N$. The parameter J is the interaction amplitude and η is a measure of the symmetry of the matrix $\mathbf{J} = [J_{ij}]$. Values $\eta = 0$ and $\eta = 1$ represent the asymmetric and the symmetric case respectively. Variable $\boldsymbol{\xi} = (\xi_1, \dots, \xi_N)$ is a Wiener process with temperature T . For the present work the Ito convention is adopted. Function g is a sigmoidal function, i.e. $g(x) = \int_0^x dx' \exp(-\pi/4x'^2)$. Therefore the vector \mathbf{x} , which at time t satisfies eq[1], functionally depends on the choice of \mathbf{J} . For $\eta \neq 0$ the latter is chosen such that its entries J_{ij} , with $i \neq j$, are:

$$J_{ij} = \sqrt{\frac{1 - \sqrt{1 - \eta^2}}{2}} \frac{J}{\sqrt{N}} Z_{ij} + \frac{\eta}{\sqrt{2} \sqrt{1 - \sqrt{1 - \eta^2}}} \frac{J}{\sqrt{N}} Z_{ij}$$

2.1. Lyapunov Exponents

Since the diagrammatic method, as reported in section 6, predicts $\langle x_i(t) \rangle \rightarrow 0$ for $t \rightarrow +\infty \forall i = 1, \dots, N$ and for any initial condition (IC) $x_i(0)$, I restricted my investigation in a neighborhood of $\mathbf{0}$ which I hypothesized belongs, for the dynamics with $T = 0$, to the basin of attraction of the origin for $\eta \lesssim 0.2$. Therefore the initial condition is chosen on the unitary N -dimensional sphere as follows: components of $\mathbf{x}(0)$ are initially drawn from a normal distribution, i.e. $x_i(0) \sim \mathcal{N}(0, 1)$ then $\mathbf{x}(0)$ is replaced by $\mathbf{x}(0)/\|\mathbf{x}(0)\|_2$. The high dimensionality of the system prevents any evaluation of the basin of attraction of $\mathbf{0}$ and, in principle, trajectories with infinitely close initial conditions may separate exponentially fast in time. Therefore the contraction and expansion of volumes in phase space, starting from the given initial condition, was tested by computing the maximum Lyapunov exponent, i.e. the following limit is supposed to exist and be finite:

$$\chi(\delta\mathbf{x}(0)) = \lim_{t \rightarrow +\infty} \frac{1}{t} \ln \left(\frac{\|\delta\mathbf{x}(t)\|_2}{\|\delta\mathbf{x}(0)\|_2} \right) \quad (2)$$

Numerically, the evaluation above made use of the Benettin algorithm [9] and it is presented in the following section. It has to be noticed that numerical simulations made over an ensemble \mathcal{J} of interaction matrices and over thermal noise give a probability density function rather than a single value for χ , i.e. $\chi = \chi(\delta\mathbf{x}(0); \eta, \mathbf{J}, T)$.

3. Direct Simulations

Numerical solutions of the Langevin equations (1) can be tackled in two different ways. Namely, according to the quantity investigated, strong and weak convergence can be required. Considering the average over the noise T , written with the braket notation, a numerical solution of 1, $\mathbf{x}_{\Delta t}(t)$, is said to be weakly convergent to $\mathbf{x}(t)$ at time t , with order p , if ([10]):

$$|\langle f_i(\mathbf{x}(t)) \rangle - \langle f_i(\mathbf{x}_{\Delta t}(t)) \rangle| = O((\Delta t)^p)$$

Where $f_i = -x_i + \sum_j J_{ij}g(x_j)$. Conversely, stating the previous hypothesis and considering each component, $\mathbf{x}_{\Delta t}(t)$ is strongly convergent to $\mathbf{x}(t)$ with order s if:

$$\langle |\mathbf{x}(t) - \mathbf{x}_{\Delta t}(t)| \rangle = O((\Delta t)^s)$$

In the present paper both of the previous notions are used. In fact in order to compute the mean $\langle \mathbf{x} \rangle$ the weak scheme can be considered sufficiently adequate. Since T is fixed, simulations were repeated N_{sim} times over the ensemble of matrices $\mathcal{J} = \{\mathbf{J}\}$ consisting of 30 randomly selected matrices for each value of η . The values of η were chosen in order to explore its domain, namely $\eta \in \{-1, -0.5, -0.2, 0, 0.2, 0.5, 1\}$. The eigenvalues of the matrices $(-\mathbb{1} + \mathbf{J})$, with \mathbf{J} belonging to \mathcal{J} , for $N = 10$ and $N = 100$, are shown in figs[2,3]. As it can be seen from figs[2d,3d] for $\eta = 0$ and for some matrices \mathbf{J} there exist an eigenvalue λ with positive real part; however, due to finite size of the system, transition becomes more evident for $\eta = 0.2$. The initial condition is kept fixed as previously reported. Approximated values $\langle \mathbf{x} \rangle$ and $\langle \mathbf{x}\mathbf{x} \rangle$ are computed considering the following weak order 2 Runge Kutta scheme ($p = 2$), if \mathbf{x} and \mathbf{x}^+ represent the value at times t and $t + \Delta t$ respectively, then:

$$\mathbf{x}^+ = \mathbf{x} + \frac{1}{2} (f(\mathbf{x}) + f(\mathbf{x})\Delta t + \delta\mathbf{W}) + f(\mathbf{x})\Delta t + \delta\mathbf{W} \quad (3)$$

Component of $\delta\mathbf{W}$ can be rewritten as $\delta W_i \sim \mathcal{N}(0, 2T\Delta t)$. For each $i = 1, 2, \dots, N$ and time $t_k = k\Delta t$, the means $\langle x_i(t_k) \rangle$ are approximated by $\bar{x}_i(t_k) = 1/N_{sim} \sum_{sim} x_i(t_k)$ while same time autocorrelations, defined for each i as $\langle x_i(t)x_i(t) \rangle$, are approximated by $\bar{x}_i\bar{x}_i(t_k) = 1/N_{sim} \sum_{sim} x_i(t_k)x_i(t_k)$. Eq[1] is supposed to be non-dimensionalised, therefore the simulations rely on the following choices: $\Delta t = 0.01$, $N_{sim} = 100$. The final time of the simulations, T_F , is set to $T_F = 15$. Conversely, following the procedure adopted by [8], the computation of the Lyapunov exponent χ requires a strong scheme, since χ in eq[2] is evaluated for every realisation of $\mathbf{x}(t)$. A deviation from a given trajectory, $\delta\mathbf{x}(t)$, satisfies $\partial_t \mathbf{x}(t) + \partial_t \delta\mathbf{x}(t) = f(\mathbf{x}(t)) + \partial_x f \delta\mathbf{x}(t) + \xi(t)$, therefore $\partial_t \delta\mathbf{x} = \partial_x f(\mathbf{x}(t))\delta\mathbf{x}$. Since ξ is not a function of \mathbf{x} the previous weak scheme can be used as a strong one with $s = 1$, i.e. it represents an acceptable numerical compromise in order to compute χ . Due to high computational requirements, the number of matrices belonging to the ensemble \mathcal{J} considered in the computation of χ is reduced to 10 for each η when $N = 100$. Exponent χ is computed by using the Benettin algorithm as follows: the initial perturbation is chosen on the N -dimensional sphere, i.e. $\sum_{i=1}^N \delta x_i^2(0) = 1$ while the variational equation is $\partial_t \delta\mathbf{x} = (\mathbb{1} + \mathbf{J} \cdot \nabla g(\mathbf{x}(t)))\delta\mathbf{x}$. Briefly, starting from an initial condition at time t such that $\|\delta\mathbf{x}(t)\|_2 = 1$ the variational problem is solved for the time interval $[t, t + \tau]$ for a fixed value of τ . At $t + \tau$ the value $\|\delta\mathbf{x}(n\tau)\|_2$ is stored and the simulation is restarted with the euclidean norm scaled again such that $\|\delta\mathbf{x}(n\tau)\|_2 = 1$. The procedure is repeated M times until the final time $T_F = M\tau$. Lastly the Lyapunov exponent is evaluated considering the stored values $\|\delta\mathbf{x}(n\tau)\|$ as follows:

$$\chi \approx \frac{1}{M\tau} \sum_{n=1}^M \ln \|\delta\mathbf{x}(n\tau)\|_2 \quad (4)$$

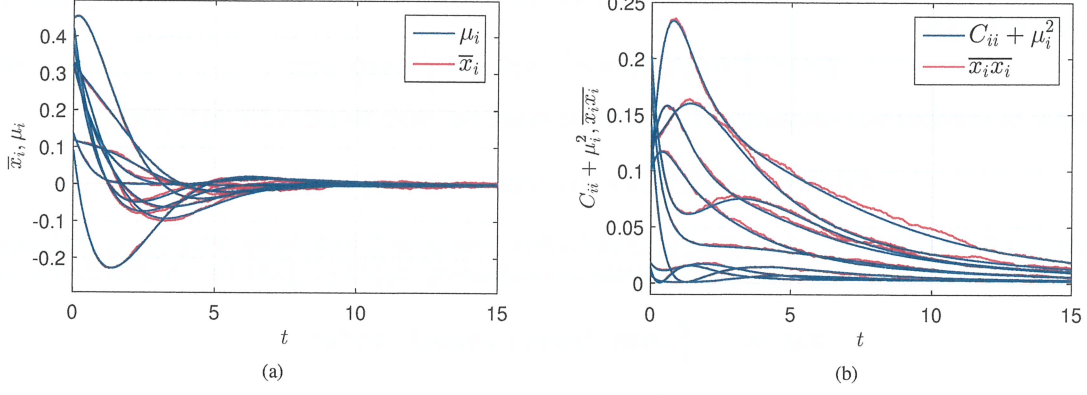


Figure 5: Detail of the numerical solution of eq[5] with $\eta = 0$ and $N = 10$.

Where $\Gamma_{ij}^{*,n+1}$:

$$\Gamma_{ij}^{*,n+1} = \sqrt{2} \sum_{r \neq i} J_{ir} C_{jr}^n \frac{1}{\sqrt{2 + \pi C_{rr}^n}} \exp\left(-\frac{\mu_r^{*2}\pi}{4 + 2\pi C_{rr}^n}\right)$$

Lastly μ_i^{n+1} is obtained from temporary solution μ_i^* and C_{jj}^{n+1} , replacing in eq[6] μ_i^* with μ_i^{n+1} , μ_i^n with μ_i^* and C_{jj}^n with C_{jj}^{n+1} (see fig[5]). Namely, the final step is $\Delta t/4 + \Delta t/2 + \Delta t/4 = \Delta t$. ICs are taken consistently with the direct simulations, i.e. $\mu_i(0) = x_i(0)$ therefore $\sum_{n=1}^N \mu_n^2(0) = 1$ while $C_{ij}(0) = 0 \forall i, j$. Additionally, it has to be noticed that there is a formal time shift between the advance in time of μ and C , therefore both of the latter are expected to be sufficiently smooth in order to assume $\mu(t + \Delta t) \approx \mu(t + \Delta t/2)$ without additional interpolations. The error introduced so far consists of two combined parts, one due to the model, since I assumed x is a multivariate Gaussian, and a second part due to the discretization and split of the ODEs. After selecting a suitable norm the error of the method is computed as the relative distance between the direct simulations and solutions of eqs[6,7] (see section 6). Clearly, also numerical solutions of eq[8] are affected by error nevertheless the latter is assumed to be sufficiently negligible since an analytical expression is not available.

5. Diagrammatic Perturbation Theory

Diagrammatic perturbations presented in this section are based on the generalisation of [13] and on [14] adopting a generating functional analysis (GPA) formalism. Functional derivatives of the generating functional \mathcal{Z} allows to compute the statistics and the moments related to the system. Therefore I proceeded as follows. Given an initial condition $x(0)$, time-discrete form of eq[1] can be written as:

$$x^{n+1} = x^n - \Delta t x^n + \Delta t J g(x^n) + \sqrt{\Delta t} \xi^n + x(0) \delta_{n,0}$$

Where superscript n represents the time $t^n = n\Delta t$. The probability density function of observing a given trajectory $\{x^n\}_{n=0}^{N_T}$ is:

$$\mathcal{P}[\{x^n\}_{n=0}^{N_T} | \xi, x(0)] = \prod_{n=0}^{N_T} \delta(x^{n+1} + (\Delta t - 1)x^n - \Delta t J g(x^n) - \sqrt{\Delta t} \xi^n - x(0) \delta_{n,0}, 0)$$

Considering the Fourier transform $\delta(z) = 1/(2\pi) \int dk \exp(-ikz)$, $\mathcal{P}[\{x^n\}_{n=0}^{N_T} | \xi, x(0)]$ becomes:

$$\mathcal{P}[\{x^n\}_{n=0}^{N_T} | \xi, x(0)] = \int \prod_{m=0}^{N_T} \frac{dk^m}{2\pi} \exp\left(-\sum_{n=0}^{N_T} k^n \cdot (x^{n+1} + (\Delta t - 1)x^n - \Delta t J g(x^n) - \sqrt{\Delta t} \xi^n - x(0) \delta_{n,0}, 0)\right)$$

White noise ξ has the probability density function which is Gaussian, i.e. $P(\xi) = 1/(\sqrt{2\pi}\sigma) \exp(-\xi^2/2\sigma^2)$ with $\sigma^2 = 2T$. Therefore $\prod_{k=0}^{N_T} \langle \exp(i \sqrt{\Delta t} k^k \cdot \xi^k) \rangle_\xi = \exp(T(i \sqrt{\Delta t} k^k)^2)$ and \mathcal{P} can be rewritten as:

$$\mathcal{P}[\{x^n\}_{n=0}^{N_T} | \xi, x(0)] = \int \prod_{m=0}^{N_T} \frac{dk^m}{2\pi} \exp\left(-i \sum_{n=0}^{N_T} k^n \cdot (x^{n+1} + (\Delta t - 1)x^n - \Delta t J g(x^n) - x(0) \delta_{n,0}) + T \Delta t (ik^n)^2\right)$$

Table 1: List of terms computed with $n \leq n^* = 5$ for the mean (a) and the correlation (b)

(a) Order n	Power of \mathcal{I}_i					(b) Order n	Power of \mathcal{I}_i				
	n_1	n_2	n_3	n_4	n_5		n_1	n_2	n_3	n_4	n_5
2	0	0	1	0	1	3	0	0	0	1	2
3	1	0	1	0	1	4	0	0	2	0	2
4	0	1	1	1	1	4	1	0	0	1	2
4	2	0	1	0	1	5	1	0	0	2	2
5	0	1	3	0	1	5	1	0	2	0	2
5	3	0	1	0	1	5	2	0	0	1	2
5	1	1	1	1	1	/	/	/	/	/	/

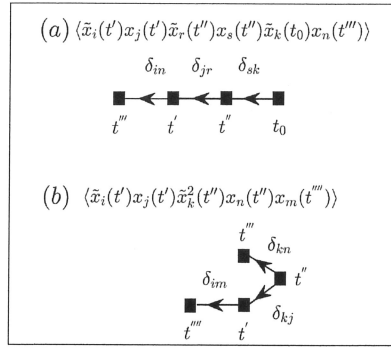


Figure 6: Example of diagrams used for the mean (a) and for the autocorrelation (b).

can associate to every \mathcal{I}_i a vector $\mathbf{v}_i = [v_{1i} \ v_{2i}]'$ where the first component v_{1i} counts the number of \tilde{x} and v_{2i} counts the number of x in the intergral \mathcal{I}_i ; namely $\mathbf{v}_1 = [1 \ 1]', \mathbf{v}_2 = [1 \ 3]', \mathbf{v}_3 = [1 \ 0]', \mathbf{v}_4 = [2 \ 0]'$ and $\mathbf{v}_5 = [0 \ 1]'$. It is straightforward now to write a code with 4 loops on (n_1, n_2, n_3, n_4) and check how many 4-tuple (n_1, n_2, n_3, n_4) satisfies $n_1 + n_2 + n_3 + 2n_4 = n_1 + 3n_2 + 1$ for the means and $n_1 + n_2 + n_3 + 2n_4 = n_1 + 3n_2 + 2$ for the correlations with the constraint on the sum $|\mathbf{n}| \leq n^*$ (table[1]). It has to be noticed that this approach does not give, in principle, the same hierarchy of terms of classical diagrammatic theory as non linear terms in \mathbf{J} and \mathbf{x} anticipate some linear terms which now appear when $n \geq n^*$. In the present work I considered $n^* = 3$, $n^* = 4$ and $n^* = 5$.

5.1. Derivation of Means

From what has been exposed so far, the means for each $i = 1, \dots, N$ are computed by evaluating the following terms:

$$\begin{aligned}
\langle \mathcal{I}_3 \mathcal{I}_5 \rangle &= \sum_i x_i(0) \int dt' \psi_i(t') G(t', 0) \\
\langle \mathcal{I}_1 \mathcal{I}_3 \mathcal{I}_5 \rangle &= \sum_{i,j} J_{ij} x_j(0) \int dt'' \psi_i(t'') \int dt' G(t'', t') G(t', 0) \\
1/2! \langle \mathcal{I}_1^2 \mathcal{I}_3 \mathcal{I}_5 \rangle &= 1/2 \sum_{n,i,j} J_{ni} J_{ij} x_j(0) \int dt' \psi_n(t') e^{-t'} t'^2 \\
\langle \mathcal{I}_2 \mathcal{I}_3 \mathcal{I}_4 \mathcal{I}_5 \rangle &= - \sum_{ij} J_{ij} x_j(0) T \pi / 8 \int dt' \psi_i(t') e^{-t'} (e^{-2t'} + 2t' - 1) \\
1/3! \langle \mathcal{I}_2 \mathcal{I}_3^3 \mathcal{I}_5 \rangle &= \pi / 12 \sum_{ij} J_{ij} x_j(0)^3 \int dt' \psi_i(t') e^{-2t'} \sinh(t') \\
\langle \mathcal{I}_1 \mathcal{I}_2 \mathcal{I}_3 \mathcal{I}_4 \mathcal{I}_5 \rangle &= \sum_{n,i,j} J_{ni} J_{ij} x_j(0) T 15 / 4 \int dt' \psi_n(t') e^{-3t'} (e^{2t'} (-1 + 2t'^2) + 2t' + 1) \\
1/3! \langle \mathcal{I}_1^3 \mathcal{I}_3 \mathcal{I}_5 \rangle &= 1/6 \sum_{n,i,j,v} J_{ni} J_{ij} J_{jv} x_v(0) \int dt' \psi_n(t') e^{-t'} t'^3
\end{aligned}$$

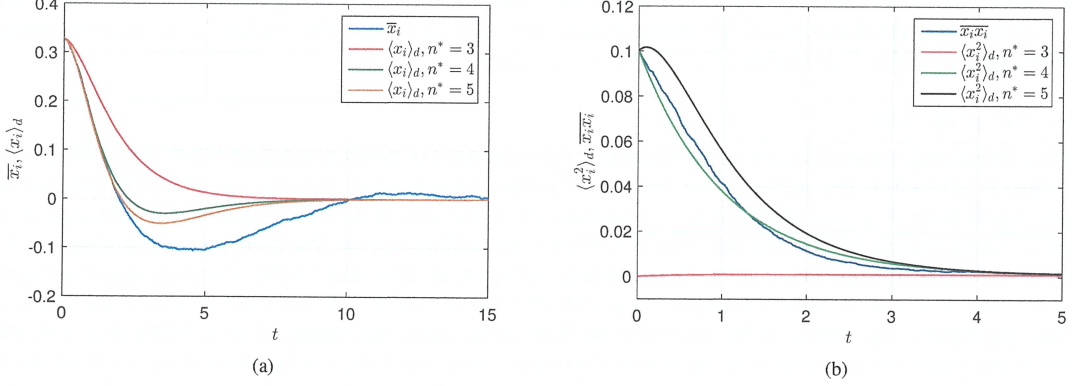


Figure 7: Detail of the diagrammatic expansion for the case $\eta = 0$ and $N = 10$ with $i = 1$.

terms, up to $n^* = 5$, can be obtained in the same manner considering $\langle \mathcal{I}_1 \mathcal{I}_4 \mathcal{I}_5^2 \rangle$ and $\langle \mathcal{I}_2 \mathcal{I}_4^2 \mathcal{I}_5^2 \rangle$. Therefore, the general for of the correlations up to $n^* = 5$ is:

$$\begin{aligned}
\langle x_i(t)x_j(t) \rangle_d &= \underbrace{2Te^{-t} \sinh(t)\delta_{ij}}_{n=3} + \underbrace{x_i(0)x_j(0)e^{-2t}}_{n=4} + \\
&+ \underbrace{T/2(J_{ij} + J_{ji})e^{-2t}(-1 + e^{2t} - 2t)}_{n=4} - \underbrace{\pi/6T^2(J_{ij} + J_{ji})e^{-2t}(-2t + \sinh(2t))}_{n=5} + \\
&+ \underbrace{\left(\sum_v J_{iv}x_v(0)x_j(0) + \sum_v J_{jv}x_v(0)x_i(0)\right)e^{-2t}t}_{n=5} + \underbrace{T12/32 \sum_v (J_{iv}J_{vj} + J_{jv}J_{vi})e^{-2t}(-1 + e^{2t} - 2t(1+t))}_{n=5}
\end{aligned} \tag{13}$$

6. Analysis of the Methods

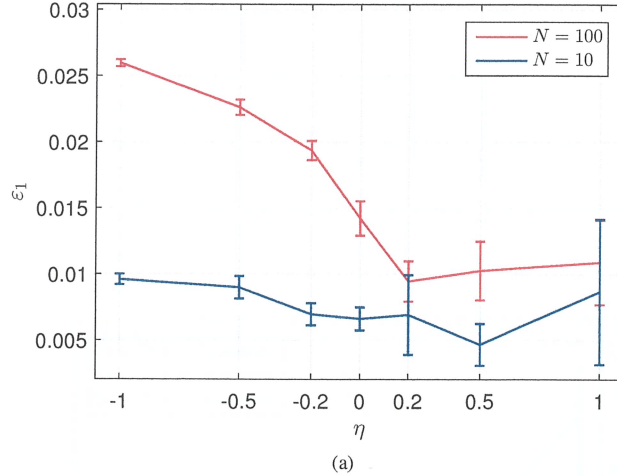
The mean and the autocorrelation for the Gaussian and for the diagrammatic approximations were compared with the mean \bar{x} and correlations $\bar{x}\bar{x}$ obtained from numerical solutions of eq[1]. Due to computational requirements for this work the number of simulation N_{sim} is set to 100 and $T_F = 15$. Therefore, with severe limitations, N_{sim} is supposed to be sufficiently high to consider \bar{x} affected by a negligible error. Then the investigation of the error for the approximations proceeded as follows. Considering the diagrammatic expansion, the partition function \mathcal{Z} in eq[9] is a Poincaré expansion; in addition, exchanging the summation $\sum_{|m|}$ with $\langle [\dots] \rangle_0$ is arbitrary as proof of uniform convergence is not provided. However, there may exist some combination of parameters (η, J, T) for which the series shows an atypical and interesting behaviour, eventually modifying its rate of divergence. In addition even if the series diverges, the time derivative of moments may have a different trend when order n^* is increased. With these premises, considering the L_1 -norm for the time interval $[0, T_F]$ I defined the following relative errors:

$$\varepsilon_1 = \left\langle \frac{1}{NT_F} \sum_{i=1}^N \frac{\int_0^{T_F} |\bar{x}_i(t) - x_i^{(\alpha)}(t)| dt}{\int_0^{T_F} |\bar{x}_i(t)| dt} \right\rangle_J \tag{14}$$

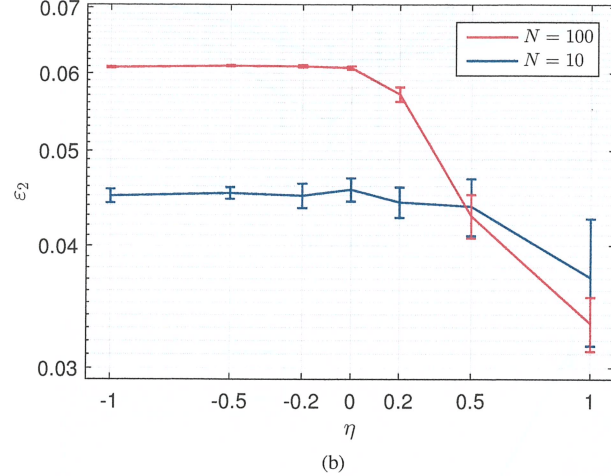
And:

$$\varepsilon_2 = \left\langle \frac{1}{NT_F} \sum_{i=1}^N \frac{\int_0^{T_F} |\partial_t \bar{x}_i(t) - \partial_t x_i^{(\alpha)}(t)| dt}{\int_0^{T_F} |\partial_t \bar{x}_i(t)| dt} \right\rangle_J \tag{15}$$

Where $x_i^{(\alpha)}(t) = \mu_i(t)$ for the Gaussian approximation and $x_i^{(\alpha)}(t) = \langle x_i(t) \rangle_d$ for the diagrammatic expansion. The same definitions of relative errors are used for the autocorrelations, replacing $\bar{x}_i(t)$ with $\bar{x}_i(t)x_i(t)$. Term $x_i^{(\alpha)}(t)$ is replaced with $C_{ii}(t) + \mu_i^2(t)$ for the Gaussian approximation and with $\langle x_i^2(t) \rangle_d$ for the diagrammatic expansion. Clearly integrals



(a)



(b)

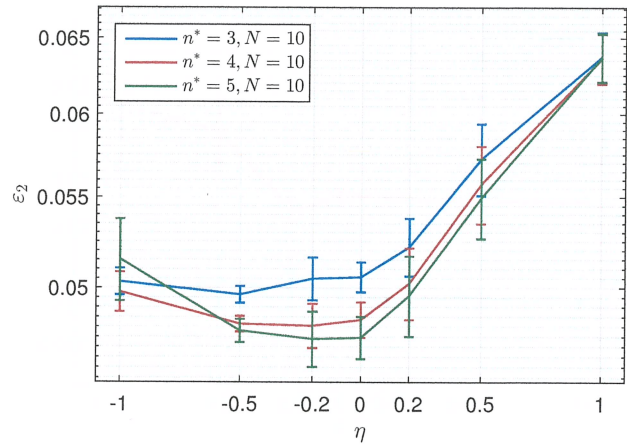
Figure 8: Relative errors ε_1 (a) and ε_2 (b) of the mean as a function of parameter η for the Gaussian Approximation for $N = 100$ and $N = 10$.

to 0.066. Curves for $n^* = 5$ and $n^* = 4$, instead, have a minimum for some negative value of η as they are convex in the interval $\eta \in [-1, 0]$. Instability of $\mathbf{0}$ makes all the approximations closer for $\eta = 1$ since:

$$\langle x_i x_i(\infty) \rangle (n^* = 3, 4) = \lim_{t \rightarrow \infty} \langle x_i x_i \rangle = T = 0.001$$

$$\langle x_i x_i(\infty) \rangle (n^* = 5) = \lim_{t \rightarrow \infty} \langle x_i x_i \rangle = T(1 + 3/4 \sum_v J_{iv} J_{vi}) \sim O(10^{-3})$$

While $\bar{x}_i \bar{x}_i(t \rightarrow \infty) = O(1)$. An anomalous trend has been found for ε_2 (fig[13](b)). In fact for $N = 100$ and $n^* = 3$ the ε_2 is a decreasing function of η . However the variation is within the interval $\varepsilon_2 \in [0.067, 0.0667]$ and $SE = O(10^{-5})$. ε_2 with $n^* = 4$ and $n^* = 5$, instead, increase up to 0.0665. The graph for $N = 10$ is completely different as all the truncations follows the same trend (fig[13(a)]). For what has been said the use of the diagrammatic expansion, at least for $n^* \leq 5$, should be confined in the interval $\eta \leq 0$. Taking into account also the description of the mean, truncations for $n^* = 5$ and $n^* = 4$ are more accurate for value of η within $[-0.5, 0]$. Since the Gaussian approximation relies on a dynamics seems to be less affected by the structure of \mathbf{J} . This is confirmed by the order of magnitude of the relative errors.



(a) $N = 10$.

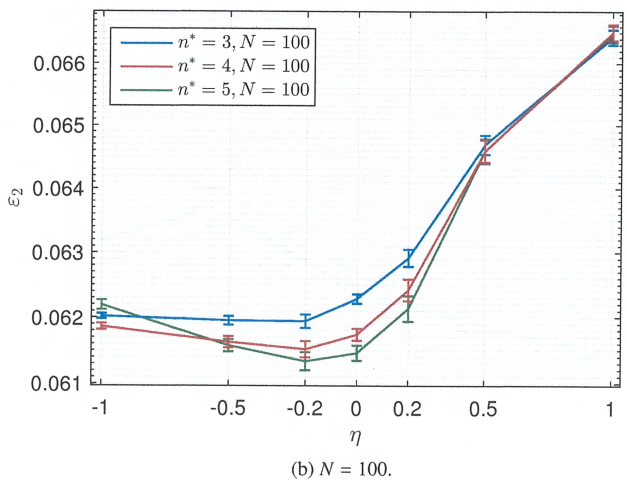


Figure 10: Relative errors ε_2 for $N = 10$ (a) and $N = 100$ (b) of the mean as a function of parameter η for the Diagrammatic expansion for $N = 100$ and $N = 10$ for different n^* .

7. Conclusions

The aim of the present work was to investigate the behaviour of the Gaussian and of the diagrammatic approximations as functions of the internal interactions of the system. The analysis of the mean and of the autocorrelations reveals that there are onset conditions for which the methods have the lowest error. While the Gaussian approximation performs excellently, the diagrammatic expansion is extremely weak as the expansion is constrained by truncation and always converges to zero for the mean. Conversely, in the light of the results, the assumption that \mathbf{x} is a multivariate Gaussian is acceptable. Autocorrelations seem extremely sensible to the parameters related to the interaction matrices as anomalous behaviour of the errors came out. The results shown are qualitatively, therefore deeper investigations should be considered. First of all, although the number of simulation N_{sim} is supposed to be sufficient, relative errors ε_1 and ε_2 are extremely sensitive to propagation of uncertainty as they contain fractions. Secondly for a full exploration of the parameter η an ensemble of 30 interaction matrices for each value of the latter is evidently not sufficient. Lastly fixing $J = 1$ made possible to qualitatively exploit theoretical results and strengthen a rigorous framework around the choice of the parameters. Further investigations could focus on $J > 1$ for which the dynamics of the free noise system is not trivial as deterministic chaoticity arises.

8. Bibliography

- [1] Peter Sollich. Theoretical Modelling of Non-Equilibrium Systems: Mission and background. *Notes for Research Methods for Theoretical Modelling of Non Equilibrium Systems, MSc Course in Non-equilibrium*, King's College London, 2017.
- [2] J. Gerald Taylor. *Mathematical approaches to neural networks*. North-Holland, 1993.
- [3] Lewis Stone, A. Roberts, M. A. Munoz, and A. Maritan. The Google matrix controls the stability of structured ecological and biological networks. *Nature Communications*, 7:12857, sep 2016.
- [4] John J Tyson, Katherine C Chen, and Bela Novak. Sniffers, buzzers, toggles and blinks: dynamics of regulatory and signaling pathways in the cell. *Current opinion in cell biology*, 15(2):221–31, apr 2003.
- [5] Gilles Wainrib and Jonathan Touboul. Topological and Dynamical Complexity of Random Neural Networks. *Physical Review Letters*, 110(11):118101, mar 2013.
- [6] Yan V Fyodorov and Boris A Khoruzhenko. Nonlinear analogue of the May-Wigner instability transition. *Proceedings of the National Academy of Sciences of the United States of America*, 113(25):6827–32, 2016.
- [7] Alexey Naumov. Elliptic law for real random matrices, <http://arxiv.org/abs/1201.1639>. 2012.
- [8] Sven Goedeke, Jannis Schuecker, and Moritz Helias. Noise dynamically suppresses chaos in random neural networks, <https://arxiv.org/abs/1603.01880>. 2016.
- [9] Giancarlo Benettin, Luigi Galgani, Antonio Giorgilli, and Jean-Marie Strelcyn. Lyapunov Characteristic Exponents for smooth dynamical systems and for hamiltonian systems; a method for computing all of them. Part 1: Theory. *Mecanica*, 15(1):9–20, mar 1980.
- [10] Timothy Sauer. Numerical Solution of Stochastic Differential Equations in Finance. In *Handbook of Computational Finance*, pages 529–550. Springer Berlin Heidelberg, Berlin, Heidelberg, 2012.
- [11] Carla Bosia, Andrea Pagnani, Riccardo Zecchina, M Caselle, and Q Huang. Modelling Competing Endogenous RNA Networks. *PLoS ONE*, 8(6):e66609, jun 2013.
- [12] Gilbert Strang. On the Construction and Comparison of Difference Schemes. *SIAM Journal on Numerical Analysis*, 5(3):506–517, 1968.
- [13] Carson C. Chow and Michael A. Buice. Path integral methods for stochastic differential equations. *The Journal of Mathematical Neuroscience (JMN)*, 5(1):8, 2015.
- [14] John A Hertz, Yasser Roudi, and Peter Sollich. Path integral methods for the dynamics of stochastic and disordered systems. *Journal of Physics A: Mathematical and Theoretical*, 50(3):033001, 2017.